

# Phase Separation in Mixed Polymer Brushes on Nanoparticle Surfaces Enables the Generation of Anisotropic Nanoarchitectures

## *Supporting Information*

Christian Rossner,<sup>\*,†</sup> Qiyun Tang,<sup>\*,‡</sup> Marcus Müller,<sup>‡</sup> and Gerald Kothleitner<sup>†</sup>

<sup>†</sup>Institut für Elektronenmikroskopie und Nanoanalytik, Technische Universität Graz, Steyrergasse 17, A-8010 Graz, Austria.

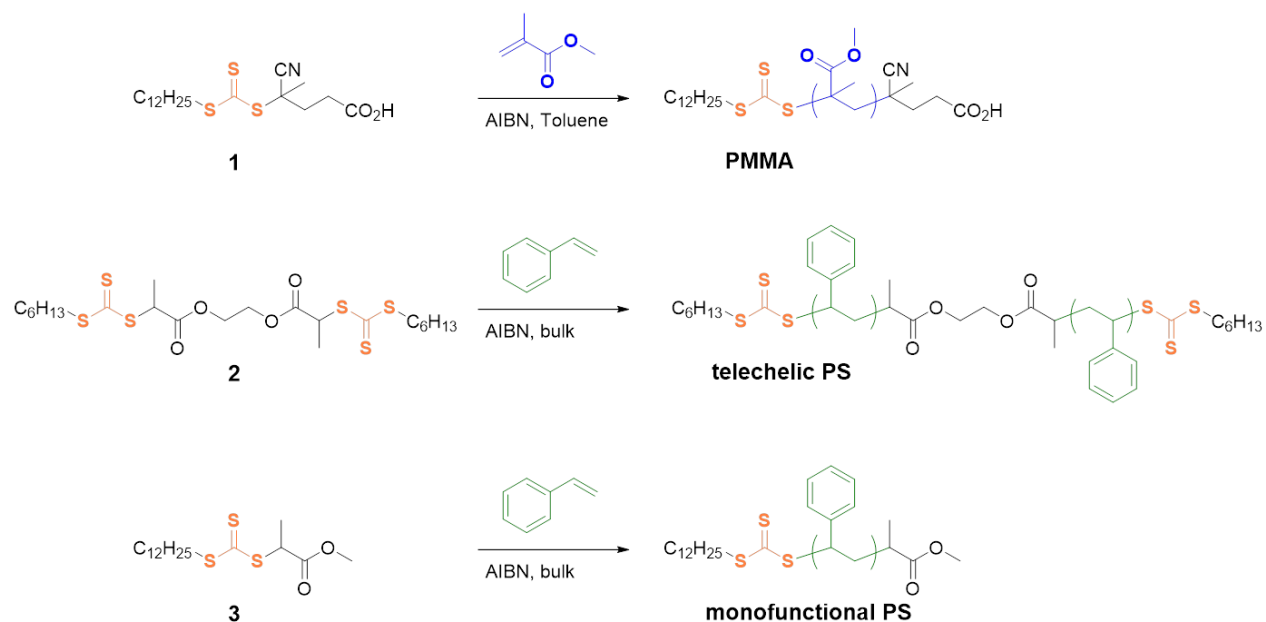
<sup>‡</sup>Institut für Theoretische Physik, Georg-August-Universität Göttingen, Friedrich-Hund-Platz 1, D-37077 Göttingen, Germany

Corresponding Authors:

\*(C.R.) E-mail: christian.rossner@felmi-zfe.at.

\*(Q.T.) E-Mail: qiyun.tang@theorie.physik.uni-goettingen.de.

## Synthetic Scheme for the performed polymerizations



**Scheme S1:** Synthetic scheme for the preparation of the different polymers used in this work.

### TEM characterization after RuO<sub>4</sub> staining

Exemplary staining experiments were performed for the core-shell particles shown in Fig. 2 in the main text. For that purpose, samples were applied onto PELCO<sup>®</sup> graphene films supported by a lacey carbon film on 300 mesh copper grids by drop casting. The sample was subsequently stained in RuO<sub>4</sub> vapor for 30 minutes at room temperature. RuO<sub>4</sub> selectively stains the PS phase.<sup>[1]</sup> TEM characterization of the stained sample was performed on a FEI T12 microscope applying an acceleration voltage of 120 kV. The experiments revealed a laterally inhomogeneous polystyrene domain, in accord with the STEM-EELS results (Fig. 2 of the main text.)

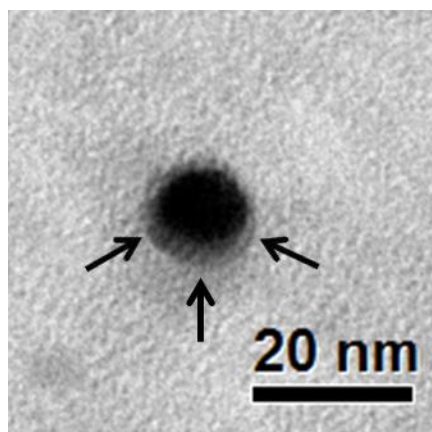


**Figure S1:** Exemplary TE micrograph of core-shell nanoparticles. The sample had been stained in RuO<sub>4</sub> vapor for 30 minutes at room temperature.

## Additional Simulation Results

### 1. Influence of solvent quality

As the Janus-like structure is prepared from solutions, the solvent quality plays a significant role for the phase behavior of mixed brushes. Here we select 3 different conditions in our simulations, corresponding to nonselective good solvents for both PMMA and PS (case I), nonselective bad solvents for both PS and PMMA (case II), and good solvent for PMMA and bad solvent for PS (case III).

**Table S1:** The cutoff of non-bonded interactions according to the solvent quality.

	$r_{\text{cut}}$ for PMMA	$r_{\text{cut}}$ for PS
Case I	$2^{1/6} \sigma$	$2^{1/6} \sigma$
Case II	$2 \cdot 2^{1/6} \sigma$	$2 \cdot 2^{1/6} \sigma$
Case III	$2^{1/6} \sigma$	$2 \cdot 2^{1/6} \sigma$

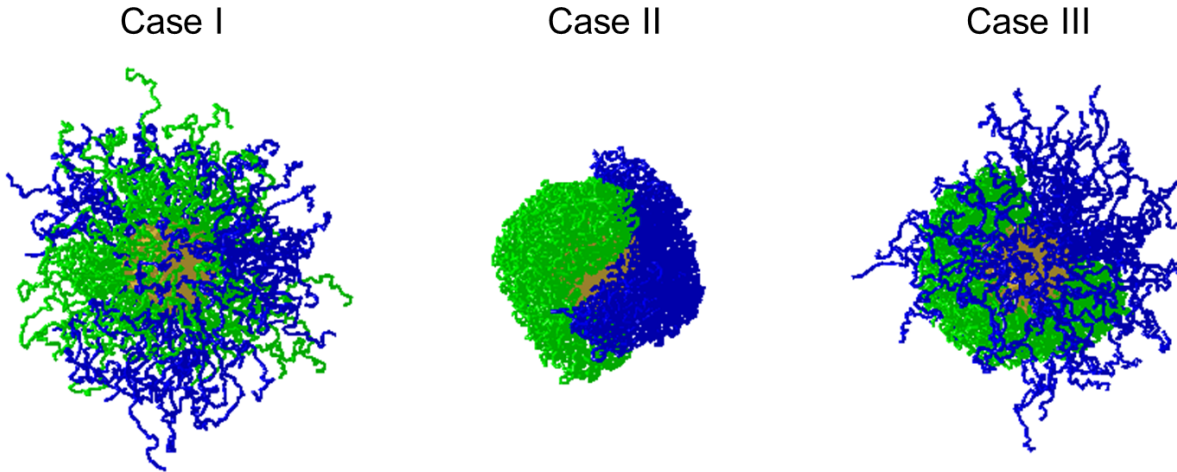


**Figure S2:** Snapshots of adsorbed PMMA and PS at different solvent qualities. The total grafting density is  $0.41 \text{ chains nm}^{-2}$  and the PS grafting density is  $0.20 \text{ chains nm}^{-2}$ . The snapshots correspond to the three cases in Table S1.

The typical snapshots of three distinct solvent qualities (see Table S1) are shown in Figure S2. It is depicted that for the nonselective good solvents, the PMMA and PS are in a weakly segregated state. The main reason is as follows: When the blend changes from melt to solution, the good solvents tend to screen/dilute the unfavorable monomer–monomer repulsion between PMMA and PS, and thus shift the critical point of phase separation. Unlike for planar polymer brushes, in our system, due to the rapid decay of monomer density as a function of distance from the surface, the critical concentration of phase transition (ODT) changes along the radial direction, giving rise to distinct morphologies of PS and PMMA on the spherical nanoparticle surface. For nonselective good solvents, the PS and PMMA monomers are less influenced by other chains in outer space due to the low density. Thus the system is in weakly segregated state at the investigated grafting density, which is obviously not consistent with experimental observations.

For the case II, the solvent is bad for both PMMA and PS. In this situation, the PMMA and PS are collapsed onto the NP surface, and form well phase-separated patterns. However, the height of PMMA is nearly the same as that of PS, and the PMMA clusters also stay on one side of the AuNP. These features are also not consistent with the experimental observations.

For case III where the solvent is good for PMMA but bad for PS, we find that the PS is collapsed onto the NP surface and tend to form clustered domains, while the PMMA distributed farther from the NP surface, with the height approx. two times larger than that of PS, see Figure 2 in the main text. These results are consistent with the experimental observations.

In total, according to the spectrum image maps observed in experiments, and compared to the different snapshots at distinct solvent conditions, we conclude that during the preparation of adsorbed PMMA and PS, the solvent quality should be weakly unfavorable to PS but slightly favorable to PMMA, which is consistent with the experimental conditions during the fabrication of hybrid particles.

## 2. Influence of grafting point mobility

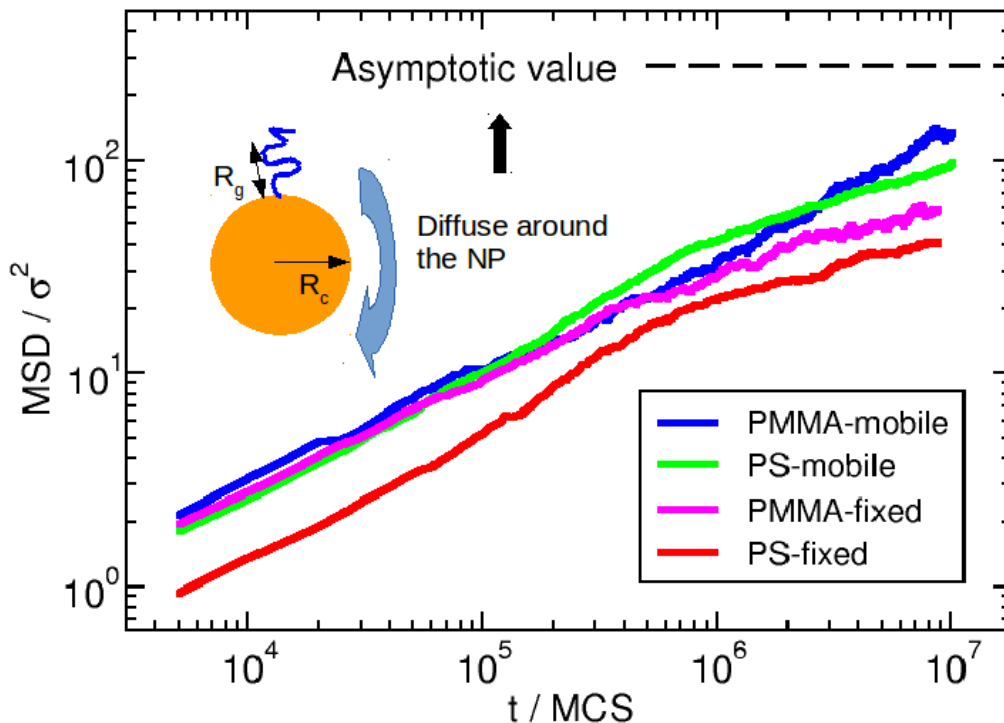


**Figure S3:** Mean-square displacements of adsorbed PMMA and PS on the AuNP surface. The grafting points are mobile and fixed. The inset shows the maximum diffusion distance of chains on the AuNP surface.

Figure S3 shows the mean-square displacements (MSD) of adsorbed PMMA and PS on the AuNP surface. The mean-square displacements on the spherical surface are defined as:

$$\langle (R_\alpha(t) - R_\alpha(0))^2 \rangle = \frac{1}{n_\alpha N_\alpha} \sum_{i=1}^{n_\alpha} \sum_{j=1}^{N_\alpha} [r_{ij}(t) - r_{ij}(0)]^2 \times \delta[|r_{i,\text{grafted}}(t) - r_{\text{np}}| - R_C] \times \delta[|r_{i,\text{grafted}}(0) - r_{\text{np}}| - R_C] \quad (\text{S1})$$

Here  $\alpha$  indicates the PMMA and PS components.  $n_\alpha$  and  $N_\alpha$  are the number and length of the grafted PMMA and PS chains. The two delta functions constrain that the  $i$ -th chain is grafted on the AuNP surface at time  $t$  and 0. Here,  $r_{i,\text{grafted}}$  is the position of grafted monomer of the  $i$ -th chain. Due to the grafting constraint, the MSD of PMMA and PS on the AuNP surface has an asymptotic value. The mean-square displacements of particles on a spherical surface can be calculated as<sup>[2]</sup>

$$\langle \delta r^2(t) \rangle = \langle [r_{ij}(t) - r_{ij}(0)]^2 \rangle = \frac{1}{V_d} \int d^3 r \int d^3 r' P(r, r', t) (r - r')^2 \quad (\text{S2})$$

while  $V_d$  is the volume where particles could move. As in our case, the polymers are grafted on the NP surface,  $V_d = 4\pi R^2$ , where  $R$  indicates the distance between the center of the gold NP and the center of mass for polymer in good solvents, see inset of Figure S2, thus  $R = R_C + R_g$ .

Here, the  $P(r, r', t)$  is the probability density of finding the particles at  $r$  at the time  $t$ , given the original position  $r'$ . Normally, this probability satisfies the Fokker-Planck equation, and can be solved numerically. As we are interested in the asymptotic value of MSD at long time limit, in this case the probability density becomes constant and is uniform around the NP surface. Thus  $P(r, r', t) = 1/(4\pi R^2)$ . The initial position of the particle could be anywhere on the NP surface, thus the integral of  $\int d^3 r' = 4\pi R^2$ . Once the initial position is chosen, we set it as the reference position, that is  $\theta' = 0$  and  $\psi' = 0$ . Now equation S2 can be simplified in spherical coordinates as:

$$\langle \delta r^2(t) \rangle = \frac{R^2}{4\pi} \int \sin\theta d\theta d\psi [\sin^2\theta + (\cos\theta - 1)^2] \quad (\text{S3})$$

This integral gives the asymptotic value of the mean-square displacement of  $2R^2 = 2(R_C + R_g)^2$ . The polymer radius of gyration can be calculated from simulation  $R_g \approx (25.483)^{0.5} \sigma = 5.048 \sigma$ . thus, the asymptotic MSD value can be calculated by  $2 \cdot (R_C + R_g)^2 = 2 \cdot (6.8 + 5.048)^2 \sigma^2 = 280.75 \sigma^2$ , see the dashed line in Figure S2.

The solvent quality is selected from Case III. The total grafting density is  $0.41 \text{ chains nm}^{-2}$  and PS grafting density is  $0.20 \text{ chains nm}^{-2}$ . For the mobile grafting points, the MSD of PS approaches a plateau after  $10^6$  MCS, however, the MSD of PMMA increases faster. This indicates that the PS pattern gradually approaches stationary state.

For fixed grafting points, the MSD of PMMA, which is in good solvent, is not influenced by fixed adsorbing points before  $10^6$  MCS. After  $10^6$  MCS, the MSD of PMMA becomes retarded. This originates from the constraints of fixed adsorbing points. For PS, which is in bad solvent, the fixed adsorbing points retard the MSD in the whole time scale, compared to the mobile adsorbing points.

## References

- [1] M. Vayer, T. H. Nguyen, C. Sinturel, *Polymer* **2014**, *55*, 1048–1054.
- [2] T. Bickel, *Phys. A* **2007**, *377*, 24–32.